Facial neuromuscular junctions and brainstem nuclei are the target of tetanus neurotoxin in cephalic tetanus

Federico Fabris, … , Cesare Montecucco, Marco Pirazzini

JCI Insight. 2023. https://doi.org/10.1172/jci.insight.166978.

Research In-Press Preview Neuroscience

Graphical abstract

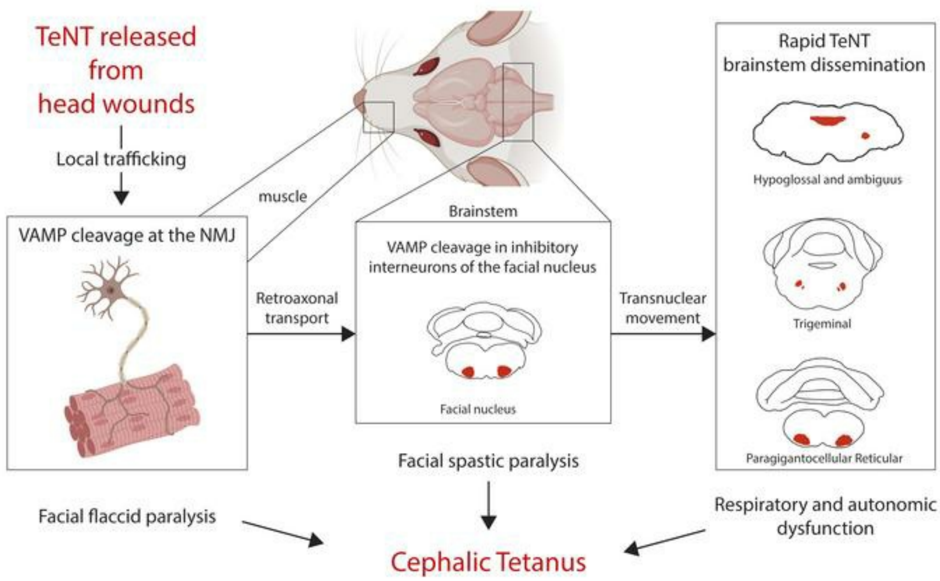

Facial Neuromuscular Junctions and Brainstem nuclei are the target of Tetanus Neurotoxin in Cephalic Tetanus

Federico Fabris[1], Stefano Varani[1], Marika Tonellato[1], Ivica Matak[2], Petra Šostaric[2], Patrik Meglic[2], Matteo Caleo[1†] Aram Megighian[1,3], Ornella Rossetto[1,4,5], Cesare Montecucco[1,4,#] and Marco Pirazzini[1,5,#]

[1]Department of Biomedical Sciences, University of Padova, Via Ugo Bassi 58/B, 35131 Padova, Italy
[2]Department of Pharmacology, School of Medicine, University of Zagreb, Šalata 11, 10000 Zagreb, Croatia
[3]Padova Neuroscience Center, University of Padova, Via Giuseppe Orus 2, 35131 Padova, Italy
[4]Institute of Neuroscience, National Research Council, University of Padova, Via Ugo Bassi 58/B, 35131 Padova, Italy
[5]Interdepartmental Research Center of Myology CIR-Myo, University of Padova, Via Ugo Bassi 58/B, 35131 Padova, Italy

[†]deceased April 12th, 2022
[#]Equal contribution as senior and corresponding authors

Corresponding authors:

- Prof. Cesare Montecucco, Institute of Neuroscience, National Research Council, Via Ugo Bassi 58/B, Padova, 35131, Italy, phone: +39 049 8276058, cesare.montecucco@gmail.com
- Dr. Marco Pirazzini, Department of Biomedical Sciences, University of Padova, Via Ugo Bassi 58/B, 35131 Padova, Italy, phone +39 049 8276058 marco.pirazzini@unipd.it

ABSTRACT

Cephalic tetanus (CT) is a severe form of tetanus that follows head wounds and the intoxication of cranial nerves by tetanus neurotoxin (TeNT). Hallmarks of CT are cerebral palsy, which anticipates the spastic paralysis of tetanus, and rapid evolution of cardiorespiratory deficit even without generalized tetanus. How TeNT causes this unexpected flaccid paralysis, and how the canonical spasticity then rapidly evolves into cardiorespiratory defects remain unresolved aspects of CT pathophysiology. Using electrophysiology and immunohistochemistry, we demonstrate that TeNT cleaves its substrate VAMP within facial neuromuscular junctions and causes a botulism-like paralysis overshadowing tetanus spasticity. Meanwhile, TeNT spreads among brainstem neuronal nuclei and, as shown by an original assay measuring the ventilation ability of CT mice, it harms essential functions like respiration. A partial axotomy of the facial nerve revealed a yet unknown ability of TeNT to undergo intra-brainstem diffusion, which allows the toxin to spread to brainstem nuclei devoid of direct peripheral efferents. This mechanism is likely to be involved in the transition from local to generalized tetanus. Overall, the present findings suggest that patients with idiopathic facial nerve palsy should be immediately considered for CT and treated with antisera to block the potential progression to a life-threatening form of tetanus.

KEYWORDS

Cephalic Tetanus; Tetanus Neurotoxin; VAMP/Synaptobrevin; Neuromuscular Junction; Brainstem; Neuroparalysis;

INTRODUCTION

Tetanus Neurotoxin (TeNT) is a 150 kDa protein released by *Clostridium tetani* during infections of necrotic wounds which causes a life-threatening neuroparalytic syndrome characterized by tonic muscle contractions and painful muscle spasticity (1-3).

Tetanus pathogenesis begins with the entry of TeNT into peripheral nerve terminals followed by retroaxonal transport and release into the spinal cord and brainstem (4-8). Therein, the toxin enters the synaptic terminals of inhibitory interneurons via synaptic vesicle endocytosis (9) and translocates its catalytic metalloprotease domain in the presynaptic cytosol (10) where it cleaves a single peptide bond of VAMP (vesicle-associated membrane protein) (11). This biochemical lesion disrupts the molecular machinery responsible for synaptic vesicle fusion with the presynaptic membrane inhibiting the release of inhibitory neurotransmitters, which in turn leads to motoneuron overexcitability and muscle spastic paralysis (5).

Tetanus can be effectively prevented via vaccination with a formalin-inactivated TeNT (tetanus toxoid) or by passive immunization with anti-TeNT immunoglobulins, which is the prophylactic therapy used with patients presenting in the emergency room with necrotic skin wounds and uncertain vaccination status (3, 8, 12, 13). Nonetheless, tetanus remains a major killer in low-income countries where vaccination and antisera availability are limited, and where the disease affects particularly newborns in the tremendous form of *tetanus neonatorum* (12-15). Novel research for non-expensive chemical inhibitors of TeNT should be encouraged (16).

The spastic paralysis of tetanus starts from the face with lockjaw (*trismus*), distortion of mouth and eyes (*risus sardonicus*), then followed by neck stiffness and trunk arching (*opisthotonos*). Spasticity progresses in a descending manner and eventually affects all muscles causing body exhaustion and patient death by a cardiorespiratory deficit (17). When a limited amount of TeNT is released in a confined anatomical area, a local form of tetanus develops with the involvement of regional muscles. This disease can then evolve into generalized tetanus depending on the further release of TeNT (2).

A rare (about 3% of cases), yet particularly dangerous form of tetanus, is cephalic tetanus (CT), which develops from infections of craniofacial wounds, of the inner ear, or mouth gingivae with *C. tetani* spores. CT begins with a peculiar botulism-like cranial nerve palsy that generally precedes, or sometimes accompanies, *trismus* and *risus sardonicus* (17-19). This unusual manifestation complicates the diagnosis of tetanus, which often goes unsuspected for days, causing an unfavorable delay in the pharmacological intervention. For this reason, CT is a form of tetanus accompanied by a poor prognosis (17), because CT patients can rapidly evolve cardiorespiratory deficits before, or even without, generalized spasticity (20-22).

How TeNT causes overlapping flaccid and spastic paralysis and how this can then rapidly evolve into cardiorespiratory defects remain unresolved aspects of CT pathophysiology.

Using a rodent model of CT based on the local injection of TeNT in the whisker pad and the use of an antibody that recognizes with high specificity TeNT-cleaved VAMP, but not intact VAMP (23), we show here that CT facial palsy is caused by the TeNT-mediated proteolysis of VAMP within the neuromuscular junctions (NMJ) of facial muscles. This action precedes and then overlaps with the canonical spastic paralysis ascribed to the TeNT activity within inhibitory interneurons of the spinal cord. We also report that specific nuclei of the brainstem are affected in CT and that TeNT can spread to other brainstem nuclei controlling critical functions, including mastication, deglutition, and respiration, via both peripheral diffusion and intraparenchymal dissemination of the toxin. These findings explain why CT can rapidly evolve into a life-threatening form of tetanus and suggest that patients presenting a facial nerve palsy of unknown origin should be immediately considered for CT and treated with the effective injection of human anti-TeNT immunoglobulins.

RESULTS

TeNT local injection in the mouse whisker pad recapitulates human CT

To study CT pathophysiology, we established an experimental model in rodents based on the local injection of TeNT into the whisker pad (WP), the group of muscles responsible for vibrissae movement in whisking animals. The WP receives sensorimotor innervation from the facial nerve and its neuromuscular activity can be recorded via live imaging of vibrissae in head-fixed animals (24), and by CMAP electromyography in anesthetized animals (25). Both techniques allow the monitoring of WP activity with time, which offers the advantage of evaluating TeNT effects in the same animal before and after toxin inoculation (Figure 1A). While naïve mice freely moved their vibrissae covering a wide angle depending on the whisking activity, TeNT-treated mice progressively loosed the ability to move the ipsilateral WP and vibrissae bent toward the jaw appearing fully paralyzed after one day, a condition persisting also at day 3 and 5 (Figure 1B; Supplementary Videos 1-4). Conversely, contralateral vibrissae were normal on day 1 but progressively stacked around their position appearing paralyzed by day 5, although differently from ipsilateral ones. To characterize the two types of paralysis, we assessed neurotransmission at the NMJ by CMAP electromyography (Figure 1C). Facial nerve stimulation in naïve mice elicited CMAP displaying a biphasic trace in both WPs, while TeNT provoked a marked reduction of maximal CMAP amplitude in the ipsilateral WPs at all time points, an indication of defective neurotransmitter release at the NMJ suggestive of flaccid paralysis. (Figure 1C). To further test this possibility, we compared the TeNT-induced paralysis with that caused by Botulinum Neurotoxin type B (BoNT/B), another clostridial neurotoxin long-known to cause flaccid paralysis by cleaving VAMP at the NMJ at the same peptide bond cleaved by TeNT (11, 23). In head-fixed mice, BoNT/B injection elicited a paralysis of the vibrissae that closely resembled the one caused by TeNT (Supplementary Video 5), and, consistently, the CMAP electromyography showed a strong decrease in amplitude (Supplementary Figure 1). Interestingly, the decrease in CMAP amplitude caused by TeNT recovered by day 5, indicating that this paralytic effect is rapidly reversible in mice. At the same time, contralateral WPs displayed no changes in CMAP traces and amplitude as it occurred in naïve mice indicating that TeNT produced its local effect only in injected muscles.

Altogether, these results suggest that the action of TeNT at the NMJ is similar to the one of botulinum neurotoxins, does not cause degeneration of the motor axon terminals nor the death of the motoneurons, and it is rapidly reversed (8, 26, 27). This botulism-like paralysis in injected muscles is then followed, in a few hours, by the canonical spastic paralysis of other head muscles, found here in the contralateral whisker pad muscle. These findings are reminiscent of what occurs in human CT in patients manifesting simultaneously a flaccid and spastic paralysis of facial muscles (please see (19) for a direct comparison), thus qualifying this mouse model for the study of the molecular pathogenesis of CT.

CT flaccid paralysis is caused by the TeNT-mediated cleavage of VAMP within motor axon terminals of facial Neuromuscular Junctions

Based on CMAP findings, we hypothesized that CT nerve palsy could derive from the direct activity of TeNT at the NMJs of the WP muscle. To test this possibility, we isolated the ipsilateral and contralateral WPs at different time points after TeNT injection and stained the muscles with an antibody that specifically recognizes VAMP only after TeNT proteolysis (hereafter indicated as cl-VAMP), but not before cleavage (23). The post-synaptic membrane of the NMJs was stained with fluorescent α-Bungarotoxin which binds tightly to nicotinic acetylcholine receptors (AChR). WP injected with saline did not show cl-VAMP staining (Figure 2A), similarly to WPs contralateral to the injection side, throughout the entire time course of TeNT intoxication (Figure 2B and Supplementary Figure 2A). Conversely, a clear staining of cl-VAMP appeared in the ipsilateral WPs (Figure 2C). This signal was localized within presynaptic terminals and associated with synaptic vesicles, as indicated by its colocalization with the vesicular acetylcholine transporter (VAChT), a protein marker of these organelles (Figure 2D). Consistently with the time course of CMAP amplitude, NMJ staining quantification showed that the number of cl-VAMP positive synapses peaked at day one and then gradually decrease with time (Figure 2E).

To monitor the correlation between VAMP cleavage and flaccid paralysis, a dose dependence was performed by injecting increasing doses of TeNT. A dose of 0.25 pg/g did not cause evident cleavage of VAMP at the NMJ (Supplementary Figure 2B and 2C) and, consistently, CMAP amplitude was not altered (Supplementary Figure 2D), indicating that TeNT did not cause flaccid paralysis at this dosage. At the same time, injected animals developed spastic paralysis about 2 days after injection. At 0.5 pg/g, TeNT caused a VAMP cleavage lower than the one obtained with 1 pg/g. In parallel, CMAP showed an intermediate decrease in amplitude, indicating that there is a correlation between VAMP cleavage at the NMJ and TeNT-induced flaccid paralysis. Together with the progressive loss of cl-VAMP staining accompanying the functional recovery at day 5, these results also suggest that the reversible nature of TeNT paralysis at the NMJ depends on the degradation of the TeNT light chain within axon terminals and turnover of cleaved SNARE proteins, as reported for the other botulinum neurotoxins (27-29).

To provide further evidence that VAMP cleavage causes TeNT-induced flaccid paralysis, we extended the experiment to rats. This species carries a point mutation at the cleavage site of VAMP-1 rendering it resistant to TeNT proteolysis (Figure 3A). This is an effective biochemical knock-in model (23, 30). Rats have long vibrissae whose movements can be simply and easily monitored via video recording with a high-speed camera (Supplementary video 6). We examined their movements from proximal and distal positions with respect to the caudal part of the body (Figure 3B). These two positions were identified both in naïve rats (Figure 3C) and in injected rats on day one (Figure 3D, left panel and Supplementary video 7), suggesting that vibrissae movements did not display obvious alterations in both injected and non-injected WPs. At variance, ipsilateral whiskers began to remain stacked in between the distal and proximal positions on day 3 and appeared fully paralyzed by day 5 (Figure 3D, central and right panels, and supplementary video 8-9). To discriminate whether paralysis was flaccid or spastic, we performed a CMAP analysis. Both injected and contralateral WPs displayed a normal neuromuscular transmission, indicating a spastic paralysis (Figures 3E and 3F). Consistently, we failed to detect the staining of cl-VAMP in the motor axon terminals of injected WP (Figure 3G).

Altogether, these results show for the first time that TeNT can cleave VAMP in the cytosol of peripheral motor axon terminals causing (in susceptible species) a reversible flaccid paralysis similar to that caused by botulinum neurotoxins.

The peripheral effect of TeNT at the NMJ is dominant on its central activity within inhibitory interneurons in the FN

The above results account for the molecular origin of CT facial palsy. Yet, the cardinal and most dangerous symptom of CT is the spastic paralysis of the head and facial muscles, rapidly followed by dysfunction of swallowing, respiration, and heart function (17, 18, 21). Accordingly, the brainstem areas corresponding to these essential physiological functions, suspected to be affected by TeNT proteolysis, were studied by monitoring VAMP cleavage as a function of time after TeNT inoculation in the WP (Figure 4A). As soon as one day after injection, a strong signal of cl-VAMP appeared at the level of the ipsilateral facial nucleus (FN) containing the motor efferents of the whisking musculature (Figure 4B) (31, 32). Consistent with a presynaptic action within inhibitory interneurons, we found the staining of GlyT2, the presynaptic plasma membrane transporter of glycine, around the cl-VAMP signal (Figure 4C), which appeared as puncta colocalizing with the signal of an antibody specific for VGAT, the vesicular transporter of GABA and Glycine (Figure 4D). This staining suggests that VAMP cleavage occurred within the presynaptic space of axon terminals of inhibitory interneurons, where VAMP is localized on synaptic vesicles. The colocalization between cl-VAMP and VGAT was extensive but not complete (Figure 4E), yet some cl-VAMP puncta were not associated to this marker of inhibitory interneurons. This finding indicates that TeNT could also enter in the presynaptic space of non-glycinergic and non-GABAergic neurons, whose origin and contribution to the development of tetanus spasticity remain to be established.

With time, the intensity and occupancy of the cl-VAMP signal in the FN progressively increased, and some staining started to be visible by day 3 also in the contralateral FN. Of note, such a faint signal (compared to ipsilateral FN) was sufficient to cause muscle spasticity in the contralateral (non-injected) WP and, similarly, at day 5, suggesting that TeNT-induced muscle spasticity is determined by a comparatively limited amount of VAMP cleaved. Accordingly, considering the strong cl-VAMP signal in the ipsilateral FN, we postulated that the effect of TeNT at the NMJ causing the nerve palsy is dominant on the central activity on inhibitory interneurons associated to muscle spasticity.

TeNT central activity diffuses throughout brainstem nuclei causing respiratory dysfunction before systemic spasticity

On day 1, VAMP cleavage was mainly confined in the ipsilateral FN, but Figure 5A shows a weak staining also in the Paragigantocellular Reticular Nucleus (PGRN), a brainstem area located caudally just behind the FN containing neuronal nuclei involved in the control of respiration and autonomic cardiovascular functions (Figure 5A right panels) (33, 34). Moreover, by day 3 VAMP cleavage was detected also in the trigeminal motor (TM), hypoglossal (HN), and ambiguus (NA) nuclei, i.e., brainstem areas controlling mastication, swallowing, and more broadly the activity of the upper respiratory tract (larynx and pharynx). Of note, cl-VAMP staining significantly increased at day 5 in all these nuclei, but not elsewhere, suggesting that TeNT diffusion within the brainstem remained localized and specific.

Given that the PGRN, the HN, and the NA are involved in the control of the upper airways function and of respiration, we wondered whether TeNT action in these nuclei could cause any change in breathing. To answer this question, we took advantage of an electrophysiological assay that allows one to measure the intraesophageal pressure in living mice (Figure 5B and C); this provides an accurate estimation of the intrapleural pressure, and thus, indirectly, of the air volume exchanged by the animal during the respiratory cycle. Of note, this technique is minimally invasive allowing repeated measurements in the same animal, before and after toxin injection (35).

The top panel of Figure 5C shows the normal respirogram of a mouse before toxin treatment. One day after TeNT injection in the WP, when the cleavage of VAMP is confined in the FN, we detected little, if any, change in the mouse respirogram. Conversely, when TeNT activity spread to PGRN, HA, and NA at day 3, the variations of intraesophageal pressure at each ventilation act were markedly reduced, consistently with a defect in the mouse ability to breath. To provide a quantitative estimation, we calculated an “inferred ventilation index” (I.V.I.), i.e., a parameter indicative of the overall volume of air exchanged by the animals over 20 seconds. As shown in Figure 5D, at day 1 I.V.I. was comparable to that of naïve mice, while it decayed to about 40% at day 3 indicating a pronounced reduction in ventilation although the animal had not yet developed evident symptoms of tetanus.

Altogether, these data suggest that when TeNT reaches the central nervous system it first affects inhibitory interneurons impinging on the motor efferents responsible for its retroaxonal transport, but then it traffics trans-neuronally to adjacent areas involved in the control of mastication, swallowing, and respiration causing a respiratory deficit without systemic spasticity, as it occurs in human CT (17, 18, 20, 22).

TeNT spreading in the brainstem depends on both peripheral and brainstem intraparenchymal diffusion

Intrigued by the rapid spreading of the cleaved-VAMP signal in the brainstem, we wondered how TeNT can diffuse to several groups of neurons after having been taken up by neuronal efferents innervating head muscles.

The observation that TeNT injection in one WP causes VAMP cleavage in both ipsi- and contra-lateral brainstem areas indicates that the toxin partly diffuses at the level of peripheral tissues. On the other hand, the detection of VAMP cleavage within nuclei like the PGRN, which have no sensorimotor efferents projecting to peripheral tissues, suggested that TeNT could undergo intraparenchymal dissemination after it arrives in the brainstem. To test this possibility, we exploited the particular anatomy of the two FN and set up an experiment on the *Levator Auris Longus* (LAL) muscles, two muscles of the mouse pinna used to move the ears. As shown in Figure 6A, each of the two LALs is innervated by the Posterior Auricularis nerve, i.e., one out of the several branches of the FN (Figure 6B). Upon TeNT injection between the two LALs, we induced a bilateral intoxication of both muscles that was accompanied by a clear signal of cl-VAMP in their NMJs (Figure 6C). In addition to showing that TeNT peripheral effect was not limited to the WP, this procedure allowed TeNT retroaxonal transport to the brainstem via the two facial nerves and, as a result, elicited a simultaneous bilateral cleavage of VAMP in the two FNs (Figure 6D). Also in this case, cl-VAMP initially (day 1) appeared in subnuclei of the FN populated by motoneuron-efferents of the auricularis nerve (32), but then progressively spread and reached all the areas populated by motoneuron efferents of the entire mouse snout (Figure 6E) (32). Accordingly, we performed a partial transection to disconnect all FN efferents except those of the posterior auricularis (and digastric) subnuclei (Figure 6F), and then TeNT was injected between the LALs and its activity in the FN was monitored at day 5 via VAMP cleavage. As shown in Figure 6G (central panel) the axotomized FN displayed strong staining of cl-VAMP only in posterior auricularis and digastric subnuclei, whilst the FN with the intact nerve showed cl-VAMP appearance in the whole FN. However, a more carefully inspection revealed cl-VAMP staining within axotomized subnuclei, though less intense compared to the contralateral non-axotomized FN. In particular, the signal appeared more intense in proximal areas, especially at the level of platysmal subnuclei and still detectable also in more distant subnuclei where it appeared as discrete puncta around motoneuron soma. Intriguingly, we found a similar scenario also at the level of the PGRN which showed a clear staining for cl-VAMP notwithstanding the partial axotomy of the facial nerve (Figure 6H, right panels). Considering that the PGRN does not have efferents reaching peripheral tissues but has internal connections with the Facial nucleus (36), this result strongly suggests that the spread of TeNT activity into the brainstem, in addition to peripheral diffusion, also derives from intra-parenchymal diffusion of the toxin.

DISCUSSION

The present study unravels the unique pathogenesis and contrasting symptoms of CT and discloses novel activities of TeNT within the central and peripheral nervous systems. These findings were made possible by the development of a model of cephalic tetanus based on the local injection of TeNT in the mouse head muscles and the use of a novel antibody that specifically recognize VAMP only after cleavage (23).

The first major finding is the unexpected activity of TeNT at the NMJ of facial muscles. Together with the electrophysiological analyses showing impaired NMJ neurotransmission, which extend previous electromyographical findings in patients (37, 38), the demonstration of TeNT cleavage of VAMP within facial NMJs, obtained here for the first time, discloses the molecular lesion at the basis of CT facial palsy. This symptom is a main confounding factor for CT diagnosis and is hardly associable with tetanus since TeNT toxic activity is traditionally considered to affect exclusively neurons of the spinal cord that lead to muscle contractures and spasms. Of note, TeNT local activity at the NMJ appears to be reversible. Although we did not investigate the molecular mechanism responsible for the functional recovery, it is likely that a major determinant of the persistence of TeNT paralytic action at the NMJ is the lifetime of its catalytic domain within the motor axon terminals, as it is the case for the botulinum neurotoxins (26, 27).

A second major finding is the rapidity of TeNT spreading within the brainstem as a result of both peripheral uptake and intraparenchymal dissemination. Notably, the combination of these two processes causes a broad and efficient intoxication of key neurons that control essential physiological functions, including breathing. This explains why: i) TeNT displays its maximal toxicity in the brainstem (39), ii) CT is a highly dangerous form of tetanus, and iii) CT patients suddenly and rapidly aggravate after the onset of head muscle spasticity. In addition, these results also clarify why CT can be very severe even without evolving into generalized tetanus (2, 40).

Whether the tropism for the brainstem derives from a particular affinity of TeNT for cranial nerve terminals remains to be established. Similarly, how TeNT intraparenchymal dissemination occurs, either via simple diffusion or via interneuronal consecutive cycles of retrograde transports as found for BoNT/A (41, 42), or their combination, remains unclear. Yet, connectome data shows that the FN has inputs from the ipsilateral HN, input, and output from the NA, and projections to PGRN and TM nuclei (36, 43). It is tempting to speculate that TeNT trans-neuronal trafficking privileges retroaxonal transport over the cytosolic entry also at central nerve terminals, thus supporting transnuclear spreading. Future investigations are necessary to reveal whether this mechanism contributes to the transition from local to generalized tetanus and to trismus being the initial symptom of tetanus (1-3, 15).

Another key observation of the present study is that the peripheral action of TeNT at the NMJ is dominant with respect to the activity of the toxin on inhibitory interneurons in the brainstem. This explains why nerve palsy in human CT can persist as a unique symptom for several days before head-muscle spasticity, which then manifests suddenly and progresses to life-threatening symptoms in a short time (17, 20-22). Indeed, the peripheral effect first affects the muscles around the TeNT release site overshadowing the onset of spasticity; meanwhile the toxin has the time to spread and intoxicate large portions of the brainstem. Arguably, this is the culprit factor responsible for the delay in CT diagnosis and the ensuing fast deterioration of patients' conditions requiring intensive care (20-22).

In conclusion, the findings of the present paper suggest that patients presenting with an idiopathic facial nerve palsy should be immediately considered for a diagnosis of CT and accordingly treated with anti-TeNT immunoglobulin, when a skin, gingival or inner ear lesions are present. This procedure is well-established, innocuous, and non-expensive, yet it is capable of preventing the nefarious consequences of tetanus. In light of this, purified monoclonal antibodies with high neutralization activity injected intrathecally in the cerebrospinal fluid in the brainstem could represent a strategy with even better therapeutic outcomes than the intramuscular one (8, 44).

METHODS

Antibodies, reagents, and toxins

TeNT was purified from *C. tetani* Harvard strain cultures and was kept at -80°C (45). When injected in vivo, the toxin was dissolved in physiological solution plus 0.2% gelatin (G2500, Sigma Aldrich). An affinity-purified antiserum specific for TeNT-cleaved VAMP was obtained as recently described (23), anti-VAChT (1:500, 139 105), anti-intact VAMP-2 (1:500, 104 211) and anti-VGAT (1:500, 131 308) antibodies were purchased from Synaptic System; anti-GlyT2 (1:500, AB1773) was purchased from Chemicon; α-bungarotoxin Alexa488-conjugated (1:200, B13422) and anti-guinea pig Alexa488-conjugated (1:200, A11073) were purchased from Thermo Scientific. Anti-rabbit Alexa555-conjugated (1:200, A21428) was purchased from Life Technologies.

Ventilation recordings.

Recordings were performed before (t_i) and 24 and 72 hours after intoxication with 1 ng/kg of TeNT (diluted in 3 μl physiological solution containing 0.2% gelatine). Animals were anesthetized (xylazine/zoletil 48/16 mg/Kg). A bottomed plastic feeding tube (20 ga x 38 mm, Instech Laboratories) was carefully introduced into the oral cavity and placed in the esophagus at the level of the mediastinum. Mice were laid on the left side on a pre-warmed heat pad. Pressure variations were recorded via a pressure sensor (Honeywell, 142PC01D) connected to an amplifier. Traces were digitized with WinEDR V3.4.6 software (Strathclyde University, Scotland) and analyzed with Clampfit (Axon, USA). We inferred the volume of exchanged air by measuring esophageal pressure variations, which reflect intrapleural pressure variations (46). At least 120 epochs were recorded and at least 20 epochs were used for the analysis at each time point. The I.V.I. parameter was calculated for each animal as the product of the mean area of the peaks multiplied by the number of peaks within 20 seconds. Data represent the percentage of t_0 taken in the same animal.

Whisking behavior

Whisking behavior in mice was recorded in awake individuals head-fixed with a custom-made head plate implanted onto the skull. Briefly, animals were anesthetized (Isoflurane, Abbott Laboratories, USA), laid on a heating pad and eye drying was avoided with an ophthalmic solution. The scalp was shaved, locally anesthetized with 2.5% lidocaine, and disinfected with Betadine solution. An incision was made to expose the skull and the head plate was fixed with dental cement. Baytril was administered to prevent infection and the animal was allowed to recover in a wormed clean cage under monitoring to exclude signs of pain or distress. After animals recovered from the surgery (2-3 days), they were habituated to head-restrain for one week by time-increased sessions each day (47) in the setup consisting of a high-speed camera (acA800-510um, Basler, Germany) and custom-made infrared illumination. Videos were recorded at 300 Hz for 2 minutes taken before and at indicated times after TeNT injection.

For rat experiments, TeNT injections (50 pg in 0.9% NaCl 0.2% gelatin) in the WP were done under anesthesia with isoflurane. Whisking behavior was recorded with a GoPro 10 camera at 240 fps framerate and 1920/s shutter speed and evaluated by monitoring offline the videos frame-by-frame to spot the points of maximum extension and retraction of the vibrissae.

CMAP-electromyography

Animals were injected in the WP with the indicated amount of TeNT (diluted in 0.9% NaCl, 0.2% gelatine, 1 μL of volume) or vehicle only. At indicated times, the animals were anesthetized (xylazine/zoletil 48/16 mg/Kg) and CMAP was evoked by supramaximal stimulation with an S88 stimulator connected to needle electrodes (Grass, USA) placed nearby the nerve. Recording and reference electrodes (Grass, USA) were inserted into the WP and under the skin at the nose tip, respectively. The ground electrode was placed subcutaneously in the back lumbar area. Signals were digitized with an A/C interface (National Instruments, USA) and then fed to a PC for online visualization (WinEDR) and software analysis (pClamp). CMAPs were determined as average peak-to-peak intensity (in mV) from 5 supramaximal rectangular stimulation pulses (200 μs) delivered from the isolated stimulator via a two-channel amplifier (Npi Electronic, Germany). Stimulation and recording were controlled by a PC with Spike 2 software and a Micro1401-4 control panel (CED, UK).

Immunofluorescence

WP and LAL muscles from CD1 mice or WP from rats were dissected at indicated time points and fixed (4% paraformaldehyde, 30 minutes, RT). Brainstems were fixed by intracardial perfusion, collected, post-fixed overnight (4% paraformaldehyde, 15% sucrose), and then left for at least 2 days in PBS 30% sucrose. Brainstem and WP slices of 30 μm of thickness were cut with a cryostat (Leica), whilst LALs were used as whole mount staining. Tissues were quenched in PBS 0.25% NH_4Cl for 20 minutes, permeabilized, and saturated for 2 hours in blocking solution (15% goat serum, 2% BSA, 0.25% gelatin, 0.20% glycine, 0.5% Triton X-100 in PBS), and then incubated with primary antibodies for 24 hours (slices) or 72 hours (LAL) in blocking solution at 4˚C. Muscles were then washed three times in PBS and incubated with secondary antibodies for 2 hours at RT. Images were collected with a confocal microscope (Zeiss LSM900 Airyscan2) equipped with N-Achroplan (5x/0.15 Ph1 Air), EC Plan-Neofluar (20x/0.5 Air or 40x/0.45 Oil) or a Plan-Apochromat (100x/1.4 Oil) Objectives. Laser excitation, power intensity, and emission range were kept constant and set to minimize bleed-through. The colocalization analysis was performed with ImageJ (plug-in "colocalization analysis") on maximal projections of confocal images from at least three randomly chosen areas in at least three brainstem slices of the FN.

Statistics

Sample sizes were determined by analysis based on data collected by our laboratory in published studies. We used at least N = 4 mice/group for all experiments. We ensured the blind conduct of experiments. Data were displayed as means ± SD calculated with GraphPad Prism. Statistical significance was evaluated using unpaired Student's t-test or by one-way analysis of variance (ANOVA).

Study Approval

Our studies were carried out in accordance with the European Community Council Directive n˚ 2010/63/UE and with National laws and policies after approval by the local authority veterinary services of the University of Padova and the University of Zagreb.

Mice were purchased from Charles River Laboratories Italia and maintained under 12 hours–light/dark cycles in a controlled environment with water and food *ad libitum*. Rats (350–400 grams) were purchased from Inotiv and kept 2–3 per cage in a controlled environment with a 12/12 h light/dark cycle at 21–23 °C and 40–70% humidity. Food pellets and water were available *ad libitum*.

Author Contributions

Conceptualization, C.M., O.R., and M.P.; Investigation F.F., S.V., M.T., P.S., P.M., and I.M.; Data Curation, F.F., S.V., M.T., P.S., P.M., I.M., and A.M.; Supervision, C.M., M.P., A.M., M.C. and O.R.; Writing Original Draft, C.M. and M.P.; Writing, Reviewing and Editing, all authors.

Acknowledgments

This research was supported by the University of Padova "Progetto DOR 025271" (M.P.) and "Progetto DOR 205071" (O.R.), and by the Croatian Science Foundation project: HRZZ-UIP-2019-04Fs-8277.

Conflicts of Interest

The authors have declared that no conflict of interest exists

References

1. Yen LM, and Thwaites CL. Tetanus. *Lancet.* 2019;393(10181):1657-68.
2. Megighian A, Pirazzini M, Fabris F, Rossetto O, and Montecucco C. Tetanus and Tetanus Neurotoxin: from peripheral uptake to central nervous tissue targets. *J Neurochem.* 2021.
3. Thwaites CL, and Farrar JJ. Preventing and treating tetanus. *BMJ.* 2003;326(7381):117-8.
4. Brooks VB, Curtis DR, and Eccles JC. Mode of action of tetanus toxin. *Nature.* 1955;175(4446):120-1.
5. Brooks VB, Curtis DR, and Eccles JC. The action of tetanus toxin on the inhibition of motoneurones. *J Physiol.* 1957;135(3):655-72.
6. Schwab M, and Thoenen H. Selective trans-synaptic migration of tetanus toxin after retrograde axonal transport in peripheral sympathetic nerves: a comparison with nerve growth factor. *Brain Res.* 1977;122(3):459-74.
7. Salinas S, Schiavo G, and Kremer EJ. A hitchhiker's guide to the nervous system: the complex journey of viruses and toxins. *Nat Rev Microbiol.* 2010;8(9):645-55. doi: 10.1038/nrmicro2395.
8. Pirazzini M, Montecucco C, and Rossetto O. Toxicology and pharmacology of botulinum and tetanus neurotoxins: an update. *Archiv Toxicol.* 2022.
9. Matteoli M, Verderio C, Rossetto O, Iezzi N, Coco S, Schiavo G, et al. Synaptic vesicle endocytosis mediates the entry of tetanus neurotoxin into hippocampal neurons. *Proc Natl Acad Sci U S A.* 1996;93(23):13310-5.
10. Pirazzini M, Tehran DA, Leka O, Zanetti G, Rossetto O, and Montecucco C. On the translocation of botulinum and tetanus neurotoxins across the membrane of acidic intracellular compartments. *Biochim Biophys Acta.* 2015.
11. Schiavo G, Benfenati F, Poulain B, Rossetto O, Polverino de Laureto P, DasGupta BR, et al. Tetanus and botulinum-B neurotoxins block neurotransmitter release by proteolytic cleavage of synaptobrevin. *Nature.* 1992;359(6398):832-5.
12. World O. Tetanus vaccines: WHO position paper – February 2017. *Wkly Epidemiol Rec.* 2017;92(6):53-76.
13. Kanu FA, Yusuf N, Kassogue M, Ahmed B, and Tohme RA. Progress Toward Achieving and Sustaining Maternal and Neonatal Tetanus Elimination - Worldwide, 2000-2020. *MMWR Morb Mortal Wkly Rep.* 2022;71(11):406-11.
14. Thwaites CL, and Loan HT. Eradication of tetanus. *Br Med Bull.* 2015;116(1):69-77.
15. Thwaites CL, Beeching NJ, and Newton CR. Maternal and neonatal tetanus. *Lancet.* 2015;385(9965):362-70.
16. Rossetto O, Pirazzini M, Lista F, and Montecucco C. The role of the single interchains disulfide bond in tetanus and botulinum neurotoxins and the development of antitetanus and antibotulism drugs. *Cell Microbiol.* 2019:e13037.
17. Jagoda A, Riggio S, and Burguieres T. Cephalic tetanus: A case report and review of the literature. *Am J Emer Med.* 1988;6(2):128-30.
18. Kotani Y, Kubo K, Otsu S, and Tsujimoto T. Cephalic tetanus as a differential diagnosis of facial nerve palsy. *BMJ Case Rep.* 2017;2017.
19. Nascimento FA, Hammoud N, and Augusto FD. Teaching Video NeuroImages: Cephalic tetanus. *Neurology.* 2019;93(21):e1995.

20. Guyennet E, Guyomard JL, Barnay E, Jegoux F, and Charlin JF. Cephalic tetanus from penetrating orbital wound. *Case Rep Med.* 2009;2009:548343.
21. Doshi A, Warrell C, Dahdaleh D, and Kullmann D. Just a graze? Cephalic tetanus presenting as a stroke mimic. *Pract Neurol.* 2014;14(1):39-41.
22. Seo DH, Cho DK, Kwon HC, and Kim TU. A Case of Cephalic Tetanus with Unilateral Ptosis and Facial Palsy. *Ann Rehabil Med.* 2012;36(1):167-70.
23. Fabris F, Sostaric P, Matak I, Binz T, Toffan A, Simonato M, et al. Detection of VAMP Proteolysis by Tetanus and Botulinum Neurotoxin Type B In Vivo with a Cleavage-Specific Antibody. *Int J Mol Sci.* 2022;23(8).
24. Campagner D, Evans MH, Bale MR, Erskine A, and Petersen RS. Prediction of primary somatosensory neuron activity during active tactile exploration. *Elife.* 2016;5:e10696.
25. Takeuchi Y, Osaki H, Matsumine H, Niimi Y, Sasaki R, and Miyata M. A method package for electrophysiological evaluation of reconstructed or regenerated facial nerves in rodents. *MethodsX.* 2018;5:283-98.
26. Rossetto O, Pirazzini M, and Montecucco C. Botulinum neurotoxins: genetic, structural and mechanistic insights. *Nat Rev Microbiol.* 2014;12(8):535-49.
27. Pirazzini M, Rossetto O, Eleopra R, and Montecucco C. Botulinum Neurotoxins: Biology, Pharmacology, and Toxicology. *Pharmacol Rev.* 2017;69(2):200-35.
28. Zanetti G, Sikorra S, Rummel A, Krez N, Duregotti E, Negro S, et al. Botulinum neurotoxin C mutants reveal different effects of syntaxin or SNAP-25 proteolysis on neuromuscular transmission. *PLoS Pathog.* 2017;13(8):e1006567.
29. Duregotti E, Zanetti G, Scorzeto M, Megighian A, Montecucco C, Pirazzini M, et al. Snake and Spider Toxins Induce a Rapid Recovery of Function of Botulinum Neurotoxin Paralysed Neuromuscular Junction. *Toxins.* 2015;7(12):5322-36.
30. Patarnello T, Bargelloni L, Rossetto O, Schiavo G, and Montecucco C. Neurotransmission and secretion. *Nature.* 1993;364(6438):581-2.
31. Paxinos G, and Keith B. J. Franklin M. Paxinos and Franklin's the Mouse Brain in Stereotaxic Coordinates. *Elsevier Science*; 2012.
32. Komiyama M, Shibata H, and Suzuki T. Somatotopic representation of facial muscles within the facial nucleus of the mouse. A study using the retrograde horseradish peroxidase and cell degeneration techniques. *Brain Behav Evol.* 1984;24(2-3):144-51.
33. Smith JC, Abdala AP, Rybak IA, and Paton JF. Structural and functional architecture of respiratory networks in the mammalian brainstem. *Philos Trans R Soc Lond B Biol Sci.* 2009;364(1529):2577-87.
34. Machado BH, and Brody MJ. Role of the nucleus ambiguus in the regulation of heart rate and arterial pressure. *Hypertension.* 1988;11(6 Pt 2):602-7.
35. Stazi M, Fabris F, Tan KY, Megighian A, Rubini A, Mattarei A, et al. An agonist of the CXCR4 receptor is therapeutic for the neuroparalysis induced by Bungarus snakes envenoming. *Clin Trans Med.* 2022;12(1):e651.
36. Isokawa-Akesson M, and Komisaruk BR. Difference in projections to the lateral and medial facial nucleus: anatomically separate pathways for rhythmical vibrissa movement in rats. *Experim Brain Res.* 1987;65(2):385-98.
37. Garcia-Mullin R, and Daroff RB. Electrophysiological investigations of cephalic tetanus. *J Neurol Neurosurg Psychiatry.* 1973;36(2):296.
38. Fernandez JM, Ferrandiz M, Larrea L, Ramio R, and Boada M. Cephalic tetanus studied with single fibre EMG. *J Neurol Neurosurg Psychiatry.* 1983;46(9):862-6.
39. Wright EA, Morgan RS, and Wright GP. Tetanus intoxication of the brain stem in rabbits. *J Pathol Bacteriol.* 1950;62(4):569-83.

40. Rossetto O, and Montecucco C. Tables of Toxicity of Botulinum and Tetanus Neurotoxins. *Toxins (Basel).* 2019;11(12).
41. Restani L, Antonucci F, Gianfranceschi L, Rossi C, Rossetto O, and Caleo M. Evidence for Anterograde Transport and Transcytosis of Botulinum Neurotoxin A (BoNT/A). *The J Neurosci.* 2011;31(44):15650-9.
42. Antonucci F, Rossi C, Gianfranceschi L, Rossetto O, and Caleo M. Long-distance retrograde effects of botulinum neurotoxin A. *J Neurosci.* 2008;28(14):3689-96.
43. Department of Anatomy - Neuroscience Group - University of Rostock https://neuroviisas.med.uni-rostock.de/connectome/showRegion.php?id=4689.
44. Pirazzini M, Grinzato A, Corti D, Barbieri S, Leka O, Vallese F, et al. Exceptionally potent human monoclonal antibodies are effective for prophylaxis and therapy of tetanus in mice. *J Clin Investig.* 2021.
45. Schiavo G, and Montecucco C. Tetanus and botulism neurotoxins: isolation and assay. *Methods Enzymol.* 1995;248:643-52.
46. Akoumianaki E, Maggiore SM, Valenza F, Bellani G, Jubran A, Loring SH, et al. The application of esophageal pressure measurement in patients with respiratory failure. *Am J Respir Crit Care Med.* 2014;189(5):520-31.
47. Gentet LJ, Avermann M, Matyas F, Staiger JF, and Petersen CCH. Membrane Potential Dynamics of GABAergic Neurons in the Barrel Cortex of Behaving Mice. *Neuron.* 2010;65(3):422-35.

.

FIGURE LEGENDS

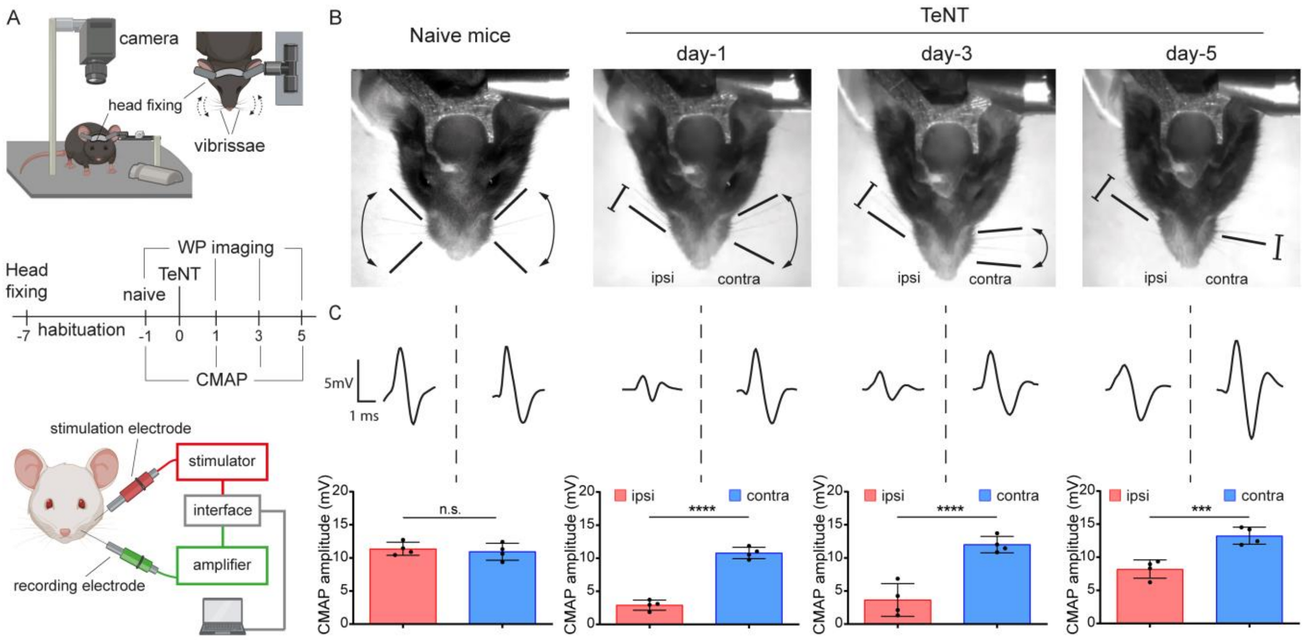

Figure 1: TeNT causes a BoNT-like flaccid paralysis upon injection in the WP in a model of CT. A) The top panel illustrates the experimental setup to video-record WP activity in head-fixed mice in a model of cephalic tetanus upon TeNT injection in the WP (1 ng/kg in a final volume of 1 µL) as a model of cephalic tetanus. Mice are held at the center of a mouse arena through a metal bar cemented to the skull; an infrared camera is positioned on top of the mouse snout to record the whisking activity. The bottom panel schematizes the apparatus to measure the Compound Muscle Action Potential (CMAP): the green electrode records WP myofibers depolarization elicited by facial nerve stimulation through the red electrode; stimulation and signal amplification are controlled with a computer connected via an interface. The central panel shows the time course of a typical experiment for WP video recording and CMAP analysis across TeNT injection in the WP. **B)** (top panels), Representative video frames showing the whisking ability in naïve mice and at indicated time points after TeNT inoculation in injected (ipsi) and non-injected (contra) WPs; black arrows and bars indicate the movement ability of the vibrissae as deduced from recorded videos; segments with blunt ends indicate full paralysis. **C)** Representative traces of CMAP recordings in ipsi and contra WP (top panels) and their quantification (bottom graphs) at indicated times after TeNT injection; Data are expressed as means ± s.d.; P values (***< 0.01; ****<0.0001) assessed by t student test. Black circles indicate the number of animals used in the experiment.

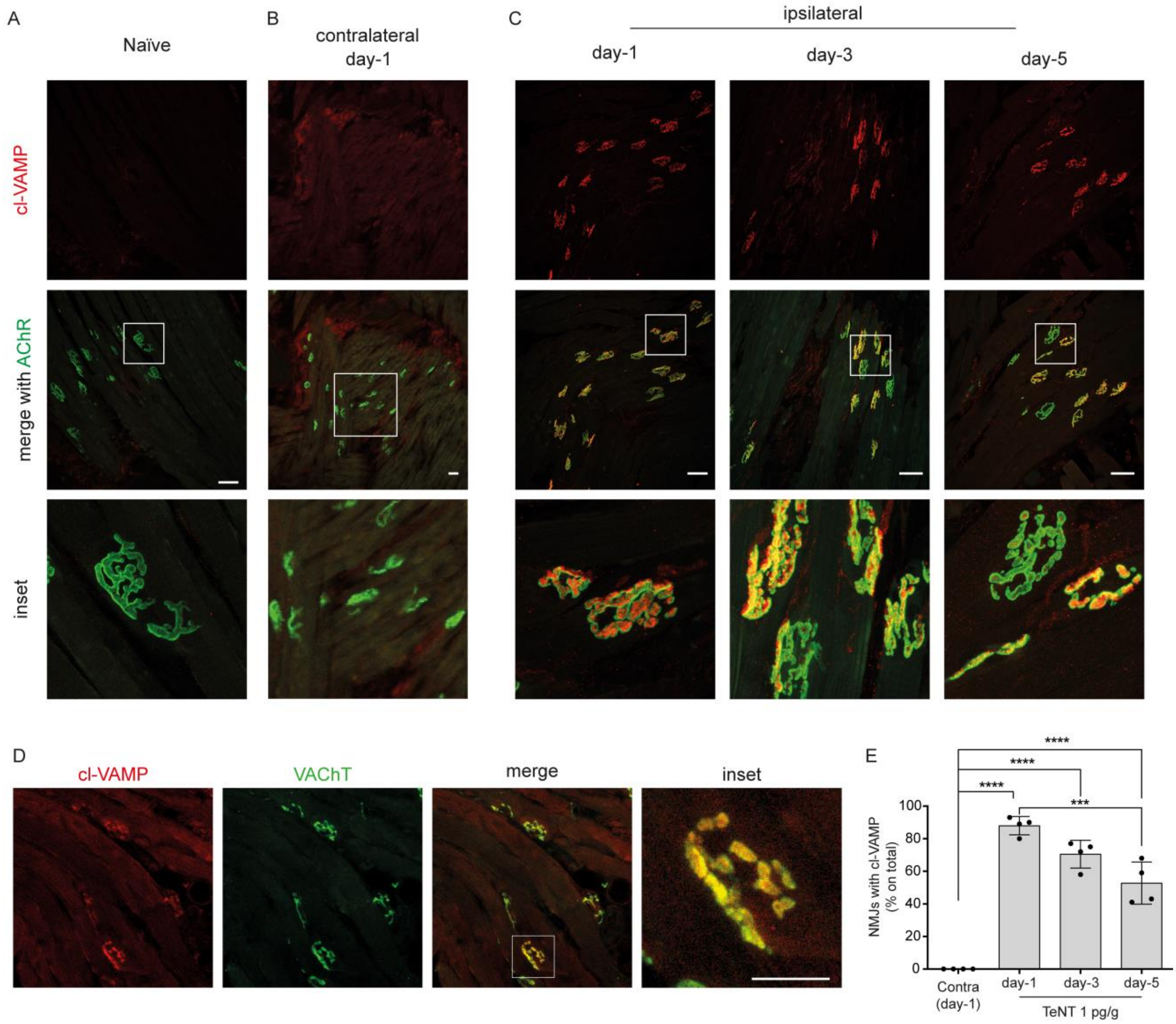

Figure 2: TeNT cleaves its target VAMP at motor axon terminals of the WP in mice. Confocal images of WP musculature from **A**) naïve and TeNT-treated mice **B**) contralateral or **C**) ipsilateral to injection at indicated times after injection; the red signal indicates the cleavage of VAMP at the NMJ identified through the labeling of nicotinic acetylcholine receptors (AChR, green) with fluorescent α-bungarotoxin; insets show a magnification. Images are representative of one from at least three independent experiments; scale bars, 50 µm. **D)** Confocal images showing colocalization between cl-VAMP (red) and the vesicular transporter of acetylcholine (VAChT, green), a protein marker of synaptic vesicles, as expected from TeNT cleavage of VAMP on synaptic vesicles at the motor axon terminal; scale bar, 50 µm. **E)** Quantification reporting the percentage of NMJs positive for the signal of cl-VAMP in the ipsilateral WP at indicated time points after TeNT injection compared to the contralateral at day one. Data are expressed as means ± s.d.; P values (***< 0.01; ****<0.0001) assessed by one-way ANOVA with Bonferroni test. Black circles indicate the number of animals used in the experiment.

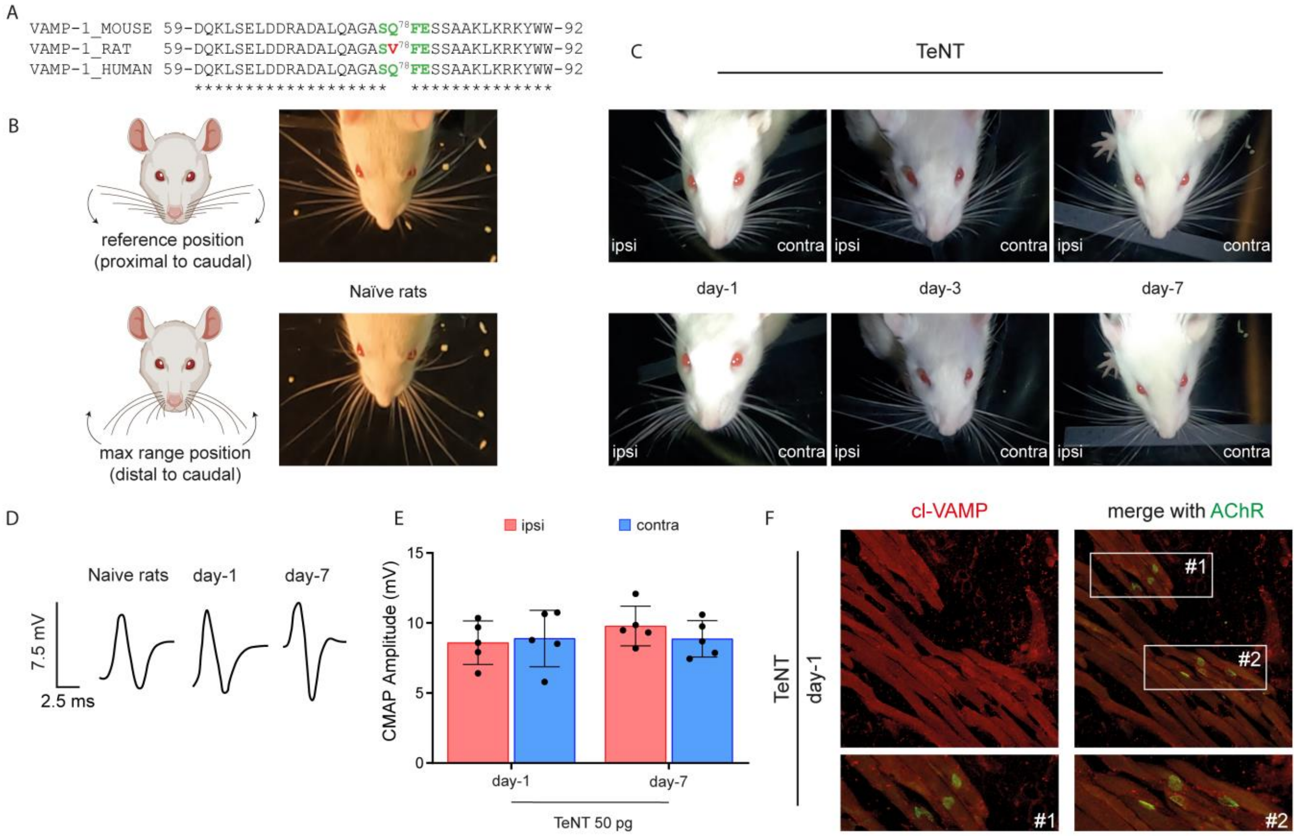

Figure 3: a point mutation in VAMP-1 renders rats resistant to TeNT peripheral neuroparalysis. **A)** Alignment showing the peptide bond cleaved by TeNT (green) in mouse and human VAMP-1 that is mutated in rats making the protein resistant to cleavage. **B)** Scheme showing the extensions of vibrissae in rats used to evaluate their whisking behaviour through video-recording after unilateral TeNT injection; top and bottom panels show the max extensions proximally and distally from the rat snout; arrows indicate the direction of vibrissae movement. **C)** Representative video frames from naïve and TeNT-treated rats at the indicated time points after TeNT injection (50 pg in total in a final volume of 10 µL) in the ipsilateral WP; top and bottom panels show that at day 1 ipsilateral whisking is normal with no flaccid paralysis, while vibrissae are stacked around their position at day 3 and day 7, suggestive of WP spastic paralysis. **D)** Representative traces of CMAP recordings at the indicated time points after the injection of TeNT in the WP, and **E**) their quantification. Data are expressed as means ± s.d. Black circles indicate the number of animals used in the experiment. **F**) Confocal images of the ipsilateral WP musculature one day after TeNT injection; the lack of cl-VAMP immunostaining indicates no TeNT activity at the NMJ identified through AChR labeling (green) with fluorescent α-bungarotoxin; insets show a magnification; images are representative of one from at least three independent experiments; bars are 50 µm.

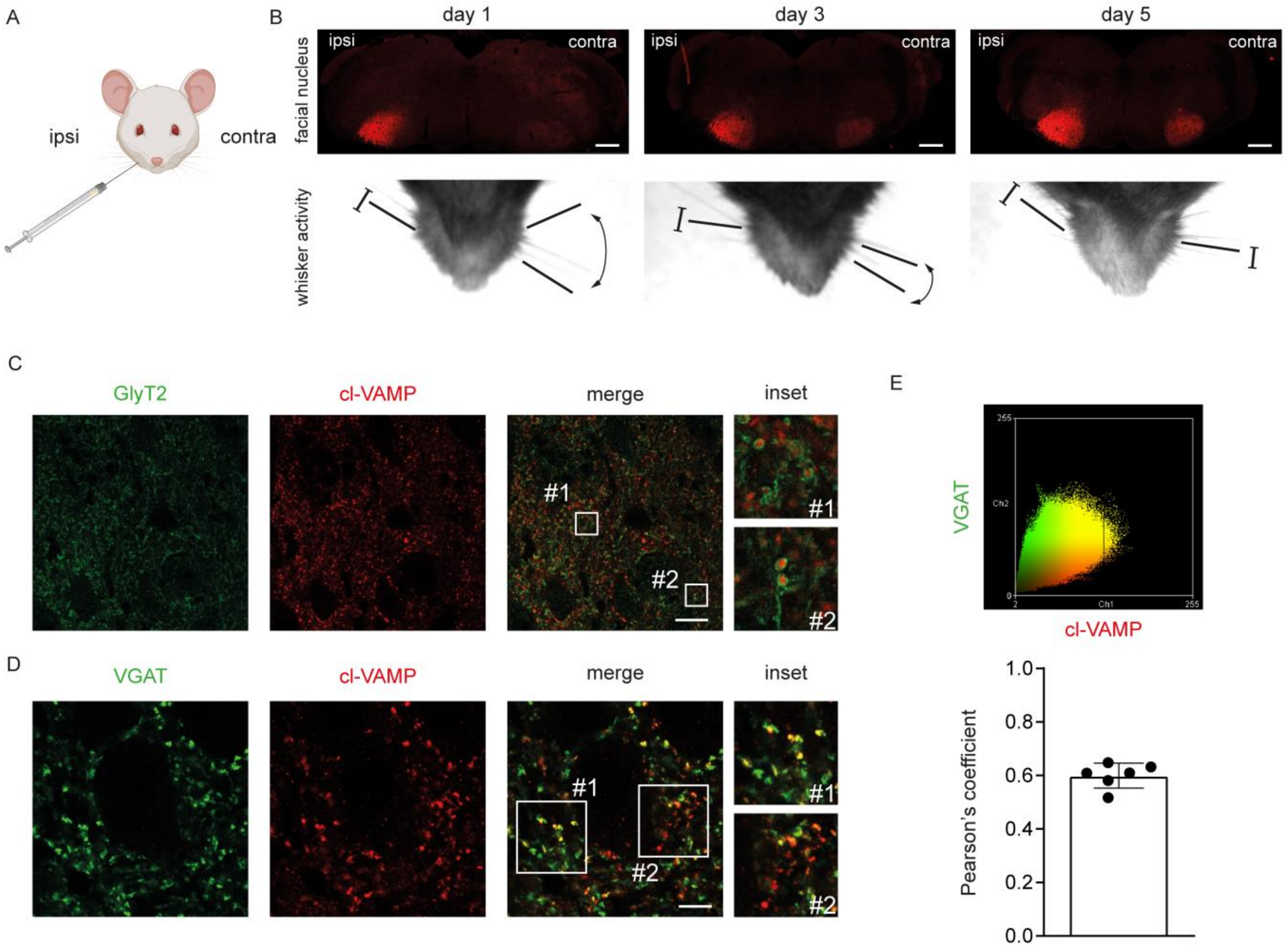

Figure 4: TeNT activity in the brainstem after injection in the WP is found at the level of inhibitory axon terminals. A) Cartoon showing TeNT injection (1 ng/kg in a final volume of 1 µL) in the WP. **B)** TeNT activity causes the appearance and progressive accumulation of cl-VAMP (red) in the facial nucleus, which acts as a reporter to illuminate the brainstem areas reached by the toxin. As soon as one day after injection, the ipsilateral FN displays a strong signal of cl-VAMP (upper panels), which increases over time although the mice still have flaccid paralysis (bottom panels). From day 3, a faint signal appears also in the contralateral side, when the non-injected WP starts to be spastic and becomes clearly stained at day 5 when the spasticity of the non-injected WP is fully attained; scale bars, 500 µm. **C)** The signal of cl-VAMP (red) is surrounded by the staining of GlyT2 (green), the plasma membrane transporter involved in the reuptake of glycine in the synaptic cleft, indicating that TeNT mainly acts within the presynaptic cytoplasm of inhibitory interneurons; scale bar, 25 µm. **D**) The signal of cl-VAMP (red) appears as puncta and colocalizes with the vesicular transporter of GABA and Glycine (VGAT, green) indicating that TeNT activity occurs specifically at the level of synaptic vesicles within inhibitory axon terminals; scale bar, 10 µm. **E**) Pearson's colocalization analysis between cl-VAMP (red) and VGAT (green) signals shown as a scatter plot (top panel) and as a histogram of the correlation coefficient (bottom panel). Black circles indicate the number of brainstem slices used for the analysis.

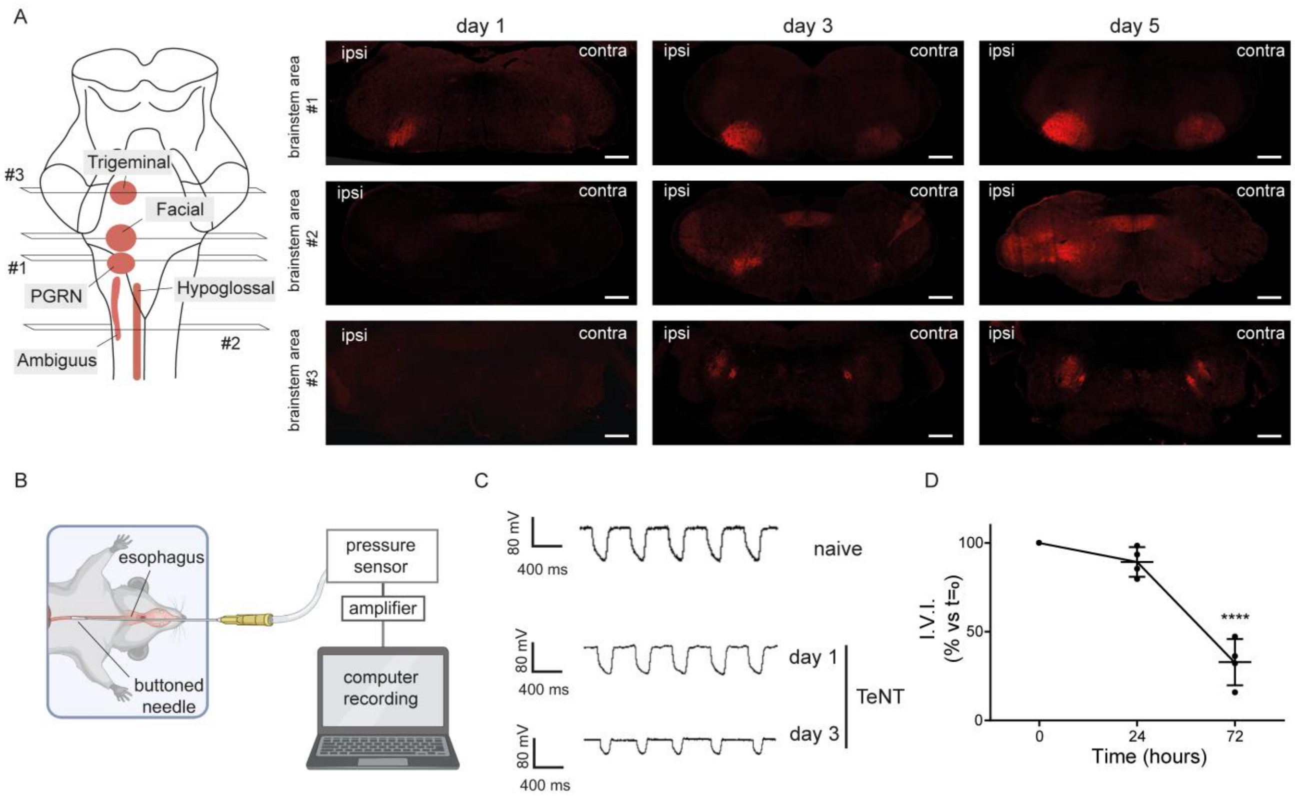

Figure 5: TeNT activity in the brainstem after injection in the WP rapidly spreads to nuclei controlling vital functions, including respiration. A) TeNT was injected in the left WP (1 ng/kg in a final volume of 1 µL) that caused the appearance of cl-VAMP (red) at the level of different brainstem areas: by day 1 the Paragigantocellular Reticular Nucleus (PGRN), involved in the regulation of respiratory and autonomic cardiovascular functions; by day 3 Trigeminal Motor (TM), hypoglossal (HN) and ambiguus (NA) nuclei, controlling mastication, swallowing and the upper airways (larynx and pharynx), respectively; scale bars, 500 µm. **B)** Scheme illustrating the experimental setup used to measure the intraesophageal pressure in living mice, which provides an accurate air volume exchanged by the animal during the respiratory cycle; a buttoned needle connected to a pressure sensor is inserted in the mouse esophagus to measure the pressure; the signal is amplified and digitalized by computer. **C)** Respirograms from naïve (top trace) and TeNT-treated mice 1 day (central trace) and 3 days (bottom trace) after WP injection. Each trace deflection reports the pressure variations occurring during a single respiratory act, which highlight the progressive reduction in the air volume exchanged during cephalic tetanus; one day after TeNT, when VAMP cleavage is confined in the FN, little if any, changes are present compared to naïve respiration; at day 3 deflections at each respiratory act appeared markedly reduced, suggesting a deterioration in the ability of the mouse to breath. **D)** Quantification of the respiratory ability reported as “inferred ventilation index” (I.V.I.) calculated as the overall volume of air exchanged by the animal over 20 seconds (see methods); data are means ± s.d.; ****= $P< 0.001$ assessed by one way ANOVA with multiple comparisons and Bonferroni test. The analysis was done with four animals per time point.

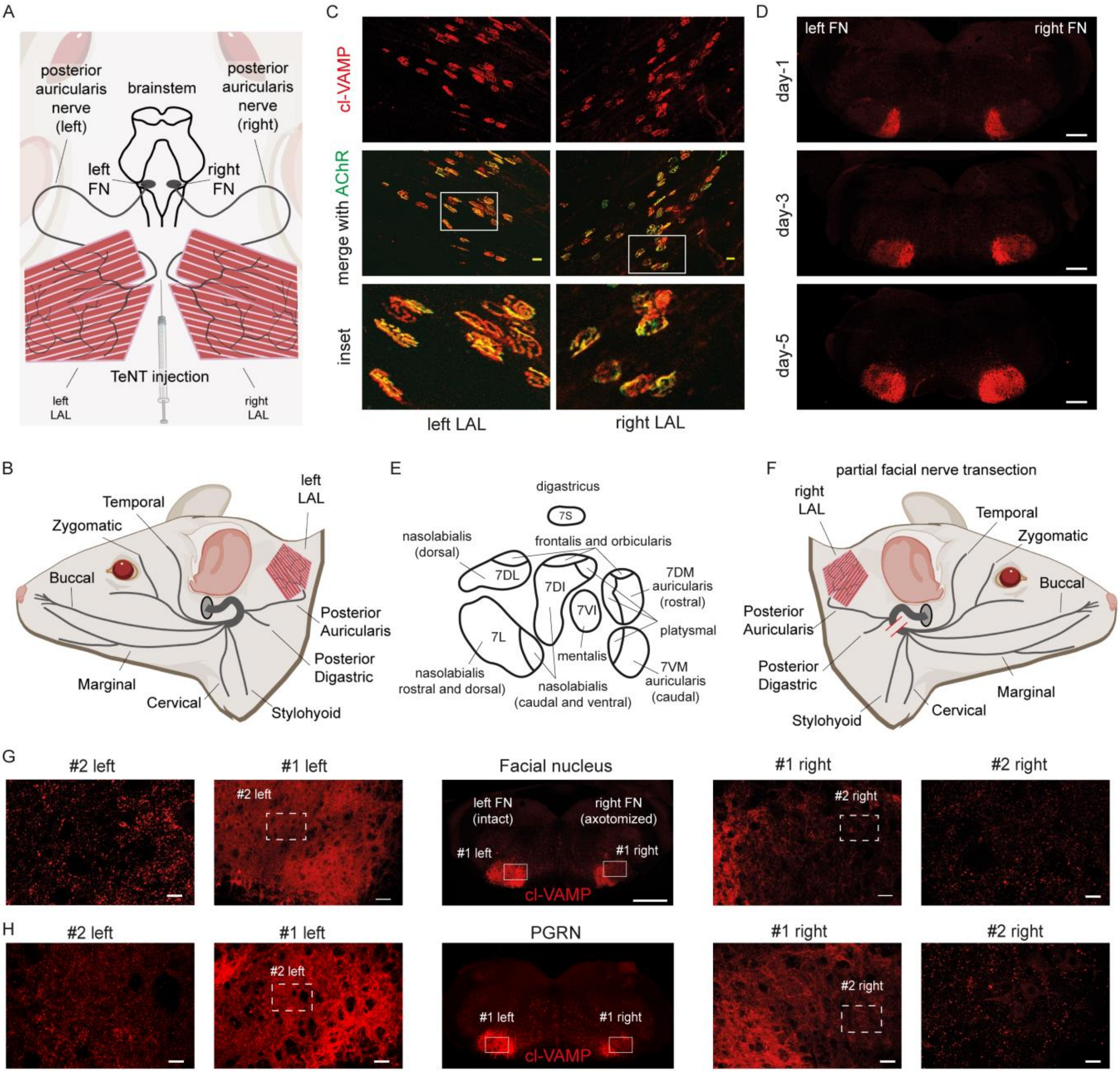

Figure 6: A combination of peripheral diffusion and intraparenchymal dissemination causes the rapid spreading of TeNT activity among brainstem neurons. A) Scheme showing the bilateral innervation of LAL muscles by the posterior auricularis branch of the facial nerve, which connects the NMJs of the left and right LAL muscles to the motoneuron cell bodies residing in the FN in the brainstem. **B)** Scheme showing how the facial nerve splits into different nerve branches that innervate the dermato-muscular system of the mouse head; each facial nerve (one per side of the head), exits at the level of the stylomastoid foramen (gray circle below the ear) and progressively divide into thinner distinct branches. **C)** TeNT injection (1 ng/kg in a final volume of 5 µL) between the two LAL muscles causes the intoxication of motor axon terminals at the NMJ level in both left and right LAL, as indicated by the staining of cl-VAMP (red) juxtaposed to AChR labeling (green) with fluorescent α-bungarotoxin. **D)** TeNT injection between the two LAL muscles leads to bilateral retroaxonal transport of the toxin via the posterior auricular branches of the two facial nerves with the ensuing appearance of cl-VAMP (red) in both facial nuclei in the brainstem; the signal appears at day 1 in the medial portions and by day 3 starts spreading toward the distal part of the FN; by day 5 cl-VAMP is found in the entire FN. **E**) Scheme reporting the subdivisions of the facial motor nucleus with reported the areas

sending axonal projections to specific muscles of the head. **F**) showing how the partial transection of the right facial nerve in the indicated position (red bars) allows disconnecting all facial branches except for the posterior auricular and digastric branches. **G-H)** TeNT injection in between the LAL muscles in mice undergoing (right) partial transection of the facial nerve causes at day 5 a different distribution of cl-VAMP staining (red) in the facial (G) and PGR (H) nuclei (central panels, scale bar 500 µm): the non-axotomized FN and PGRN display an intense signal diffused throughout the entire nucleus; the axotomized FN displays cl-VAMP signal mainly in the auricular and digastric subnuclei, but also detectable VAMP cleavage in distal FN subnuclei and PGRN appearing like discrete puncta around motoneuron soma, as shown via the progressive magnifications (#1, scale bars 50 µm); #2 scale bars 20 µm). Images are representative of one of three animals.